GEOPHYSICAL RESEARCH LETTERS, VOL. 34, L10301, doi:10.1029/2007GL029535, 2007

New constraints on the upper mantle structure of the Slave craton from Rayleigh wave inversion

Chin-Wu Chen,[1] Stéphane Rondenay,[1] Dayanthie S. Weeraratne,[2] David B. Snyder[3]

Received 3 February 2007; revised 26 March 2007; accepted 2 April 2007; published 16 May 2007.

[1] Rayleigh wave phase and amplitude data are analyzed to provide new insight into the velocity structure of the upper mantle beneath the Slave craton, in the northwestern Canadian Shield. We invert for phase velocities at periods between 20 s–142 s (with greatest sensitivity at depths of 28–200 km) using crossing ray paths from events recorded by the POLARIS broadband seismic network and the Yellowknife array. Phase velocities obtained for the Slave province are comparable to those from other cratons at shorter periods, but exceed the global average by ~2% at periods above 60 s, suggesting that the Slave craton may be an end member in terms of its high degree of mantle depletion. The one-dimensional inversion of phase velocities yields high upper-mantle *S*-wave velocities of 4.7 ± 0.2 km/s that persist to 220 ± 65 km depth and thus define the cratonic lithosphere. Azimuthal anisotropy is well resolved at all periods with a dominant fast direction of N59°E ± 20°, suggesting that upper mantle anisotropy beneath the Slave craton is influenced by both lithospheric fabric and sub-lithospheric flow. **Citation:** Chen, C.-W., S. Rondenay, D. S. Weeraratne, and D. B. Snyder (2007), New constraints on the upper mantle structure of the Slave craton from Rayleigh wave inversion, *Geophys. Res. Lett.*, *34*, L10301, doi:10.1029/2007GL029535.

1. Introduction

[2] The Slave province is an Archean granite-greenstone craton that is located in the northwest corner of the Canadian Shield and spans an area of ~600 km × 400 km (Figure 1). Several attributes make the Slave province a unique natural laboratory for detailed examination of the structure of cratonic lithosphere. It is a well-preserved craton that hosts some of the oldest rocks found on Earth, the ~4.03 Ga Acasta gneisses [*Bowring et al.*, 1990]. Furthermore, it is pierced by numerous kimberlite pipes rich in xenoliths that sample the entire lithospheric column [e.g., *Griffin et al.*, 1999]. Geochemical and petrological analyses of these mantle xenoliths reveal a distinct stratification of the Slave craton's lithosphere that is marked by variable degrees of iron-depletion and suggests an assembly by vertical stacking of subducted slabs [e.g., *Grütter et al.*, 1999; *Kopylova et al.*, 1999].

[3] A number of regional and local seismological investigations have helped characterize the vertical structure of the Slave's lithosphere. First, global and regional seismic velocity models suggest that deep continental roots extend to ~300 km depth beneath the Canadian Shield [e.g., *Grand*, 1994; *Frederiksen et al.*, 2001; *van der Lee and Frederiksen*, 2005; C. Li et al., manuscript in preparation, 2007]. However, the resolution is not sufficiently high to determine the lithospheric thickness directly beneath the Slave craton. Second, shear-wave splitting and receiver function studies have revealed the existence of azimuthal anisotropy beneath the Slave craton, but no consensus has been reached on its vertical distribution due to limitations inherent to the methods. *Bank et al.* [2000] found an average *SKS* splitting time of 1 s for the whole craton, with a fast direction of N60°E ± 20° consistent with the present-day absolute plate motion (APM) of North America. Using receiver functions, *Bostock* [1998] revealed the existence beneath the SW Slave craton of three anisotropic layers that he attributed to shallow subduction processes. More recently, *Snyder and Lockhart* [2005] suggested that only two distinct layers of anisotropy are necessary to fit azimuthally-dependent *SKS* data, with an upper layer corresponding to crustal and uppermost mantle structure, and a lower lithospheric layer influenced by plate motion.

[4] It is apparent from these results that current models lack the vertical resolution to uniquely constrain the upper mantle structure of the Slave craton. This limitation can be addressed by undertaking complementary seismic investigations such as surface wave analyses, which provide superior vertical resolution due to the waves' depth-dependent sensitivity to upper mantle structure. Here, we conduct such an analysis using a new, high-quality Rayleigh wave dataset to produce profiles of phase velocity, anisotropy and *S*-wave velocity that provide new constraints on the vertical structure of the Slave craton.

2. Data and Inversion

[5] We use fundamental mode Rayleigh wave data recorded at the POLARIS (Portable Observatories for Lithospheric Analysis and Research Investigating Seismicity) seismic network, operated by the Geological Survey of Canada, and the Yellowknife array (Figure 1). Instrument responses from different types of seismometers are normalized before data processing. The data set consists of 42 events at epicentral distances ranging between 31°–118°, with magnitudes $M_S \geq 5.5$. Rayleigh waveforms on the vertical-component seismograms are analyzed at 12 frequencies ranging from 7 to 50 mHz (20 to 142 s period). The density of crossing rays decreases with increasing period because the noise level in the data is higher at longer periods.

[1]Department of Earth, Atmospheric and Planetary Sciences, Massachusetts Institute of Technology, Cambridge, Massachusetts, USA.
[2]Department of Terrestrial Magnetism, Carnegie Institution of Washington, Washington, DC, USA.
[3]Geological Survey of Canada, Ottawa, Ontario, Canada.

0094-8276/07/2007GL029535$05.00

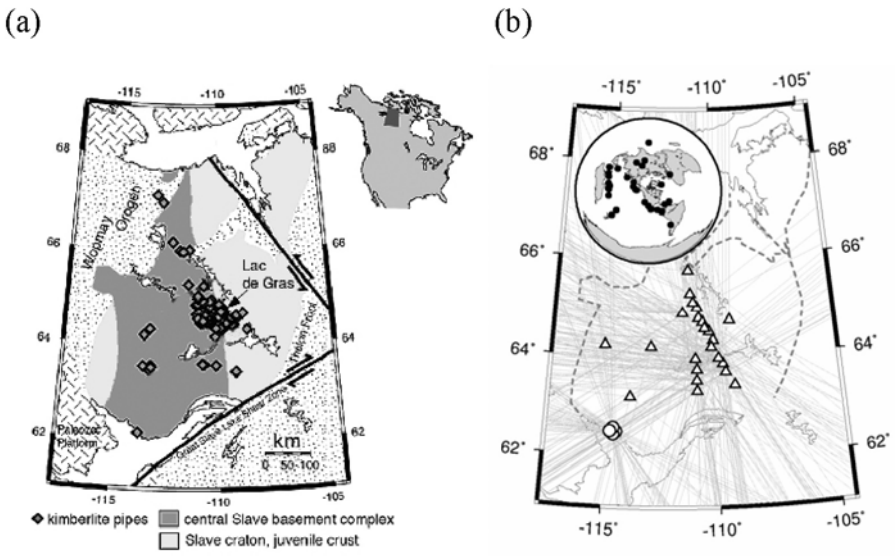

Figure 1. (a) Simplified geological map of the Slave craton and surrounding regions. The dark gray area denotes the central Slave basement complex, as defined by *Bleeker et al.* [1999]. (b) POLARIS (triangles) and Yellowknife seismic stations (circles). Dashed curves outline the boundaries of the Slave craton. Thin gray lines in the background indicate the great circle paths of events used in the inversion of Rayleigh waves at 50 s period, and represent the average ray path coverage for the entire analysis. The inset shows azimuthal distribution of 42 teleseismic events used in this study, with epicentral distances ranging between 31° and 118°.

We first filter the Rayleigh wave using a 10-mHz-wide bandpass filter centered at the target frequency, and then isolate the Rayleigh wave in a selected time window to eliminate body-wave phases and noise outside the window. The window length varies from event to event depending on the epicentral distance and dispersion characteristics, but the same window length is applied to all seismograms for a given event-frequency pair. Rayleigh wave amplitudes and phases are then determined through Fourier analysis of the filtered and windowed seismograms.

[6] A two-step procedure is adopted for the inversion of Rayleigh waves for *S*-wave velocity structure. First, Rayleigh wave amplitude and phase data are inverted for phase velocities. Second, phase velocities are inverted for *S*-wave velocity structure. In the first step, we employ the array-analysis technique developed by *Forsyth and Li* [2005], which models the incoming wave field with a two-plane-wave approximation. The method simultaneously solves for the characteristics of the incoming wave field and phase velocity, as well as anisotropic parameters, taking into account multipathing effects caused by velocity anomalies outside the seismic array. Before inverting for phase velocities, we first solve for the best fitting initial plane wave parameters for each event using a simulated annealing method while holding the velocities fixed. We then use a generalized linear inversion [*Tarantola and Valette*, 1982] that simultaneously solves for phase velocities and adjustments to the wave parameters. A detailed description of the method and successful applications are presented by *Forsyth and Li* [2005], *Weeraratne et al.* [2003], and *Li et al.* [2003].

[7] The second step of the approach involves the inversion of uniform phase velocity dispersion curve for a 1-D *S*-wave velocity profile. We use the *ak135* reference model [*Kennett et al.*, 1995] as a starting model, and search for the perturbed *S*-wave velocity model that best fits the observed phase velocities in a least-squares sense [*Weeraratne et al.*, 2003]. The predicted phase velocities are computed from *S*-wave velocity models using partial derivatives obtained through the DISPER80 package [*Saito*, 1998]. We conducted an extensive series of synthetic tests to examine the robustness of the resulting models as a function of damping parameters and starting velocity models used in the inversion. Whereas pertinent results from this analysis are invoked here in the interpretation, the full range of synthetic tests is presented and discussed in a separate paper (C.-W. Chen et al., manuscript in preparation, 2007).

3. Results

[8] Figure 2a shows the average Rayleigh wave phase velocities as a function of period obtained by inversion of the Slave craton data, along with results from selected global and regional cratonic studies (see auxiliary material for inversion results).[1] At shorter periods, between 20 and 33 s, the phase velocities increase from 3.7 to 4.05 km/s. These values are comparable to those of other cratons, such as Tanzania [*Weeraratne et al.*, 2003, and references therein]. Between 33 and 60 s, a decrease in slope is observed. At longer periods, from 60 to 140 s, the dispersion curve is generally flat with an average velocity of 4.25 km/s, but error bars do not preclude a steady increase from 4.25 km/s at 60 s to 4.4 km/s at 140 s. The average value of ~4.25 km/s is significantly higher than the average Rayleigh wave phase velocity obtained by *Brune and Dorman* [1963] for the whole Canadian Shield. It is also higher than average cratonic values from other regions (Figure 2a), e.g., eastern

[1] Auxiliary materials are available at ftp://ftp.agu.org/apend/gl/2007gl029535.

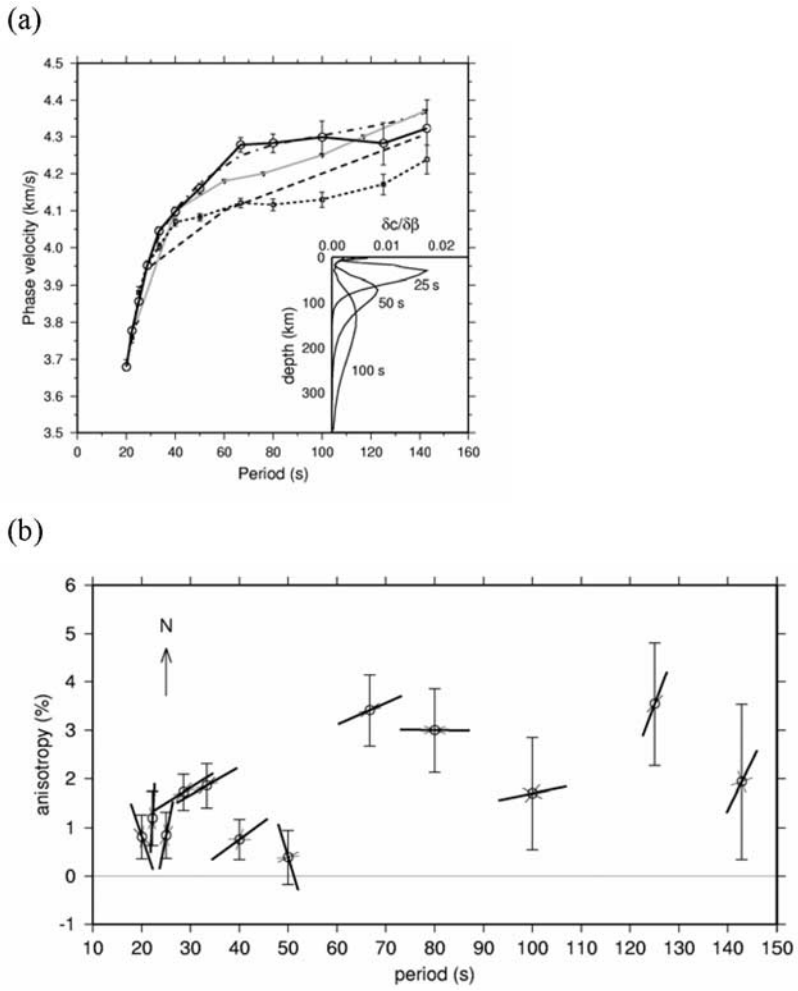

Figure 2. Results from 1-D inversion of Rayleigh waves in the Slave craton. (a) Phase velocity dispersion curve obtained in this study (black) compared to phase velocities from a surface wave study of the entire Canadian Shield (gray) [*Brune and Dorman*, 1963]; the cratonic average from a global phase velocity model (dashed) [*Ekström et al.*, 1997]; the Rayleigh wave dispersion curve for the Tanzanian craton (dotted) [*Weeraratne et al.*, 2003], and the predicted phase velocities from our model in Figure 3 (dash-dotted). Error bars indicate two standard deviations. Note that errors are small and close to the size of the symbol at short periods. The inset shows sensitivity kernels of Rayleigh waves in several periods of interest. (b) Laterally uniform azimuthal anisotropy obtained by Rayleigh wave inversion, as a function of period. Fast directions are indicated by thick black bars in map view, with gray vectors denoting two standard deviations. Vertical error bars correspond to two standard deviations of the estimated strength of anisotropy.

North America [*Li et al.*, 2003], Superior [*Darbyshire et al.*, 2007], South Africa [*Li and Burke*, 2006] (not shown), and global phase velocity models [*Ekström et al.*, 1997].

[9] By virtue of the frequency-dependent sensitivity of surface waves, the inversion also provides estimates of azimuthal anisotropy as a function of depth. In this study, we invert for uniform anisotropic characteristics beneath the Slave. The fast direction is required to be constant laterally within the craton but it is solved for independently at each period, while allowing phase velocity to vary laterally. The best fitting anisotropic parameters are shown in Figure 2b. We note that some level of anisotropy is detected at nearly all periods. The anisotropy appears to increase from an average of 1.37% at periods below 40 s to 2.7% for periods above 60 s. At periods below 29 s, the principal fast direction is N10°E ± 20°. The azimuth of anisotropy changes to a NE-SW direction of N59°E ± 20° at longer periods between 29 and 100 s. At periods >100 s, the fast direction rotates towards a N-S direction of N23°E ± 33°, with larger uncertainty.

[10] The 1-D *S*-wave velocity profile obtained by phase velocity inversion (cf. second inversion stage in data and inversion section) is shown in Figure 3. The inferred cratonic lithosphere is represented by a high velocity lid averaging 4.72 ± 0.2 km/s and extending between 50 and ~150–200 km depth. As in other cratonic areas [see, e.g., *Debayle and Kennett*, 2000; *Weeraratne et al.*, 2003], the high-velocity lid is underlain by a negative velocity gradient perhaps associated with the transition to a low-viscosity asthenospheric layer. Synthetic tests show that *S*-wave velocities are well resolved down to ~200 km depth, below which the results become more dependent on the starting model. In light of this observation, we used a set of different starting models to test the robustness of the principal

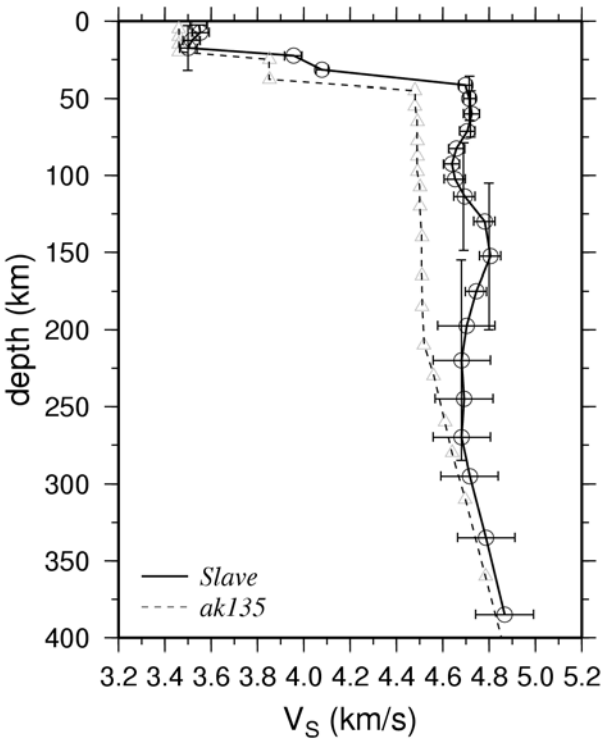

Figure 3. One-dimensional *S*-wave velocity profile (black) obtained by inversion of the phase velocity curve in Figure 2a. The starting model (dashed) is *ak135*. The horizontal error bars show the standard deviation of the resulting *S*-wave velocities at each depth. The vertical resolution, which is based on the number of adjacent layers that need to be combined to provide one independent constraint on a given velocity value, is indicated for selected depths.

features observed in the resulting profile. Results indicate that the high velocity lid between 50 and 200 km depth is resolved independently of the starting model, implying that this structure is required by the data. The presence of a high-velocity lid in this depth range is supported by continental/global-scale tomography results [e.g., *van der Lee and Frederiksen*, 2005], which show a ~4% positive (fast) anomaly in the upper mantle beneath the Slave craton relative to reference Earth models. Finally, we observe an apparent velocity reduction at ~100 km depth. However, we find that the magnitude of this anomaly is highly dependent on the level of damping used in the inversion and, consequently, that the anomaly cannot be considered as a robust feature of the model.

4. Discussion and Conclusion

[11] This study yields important new insights into the depth and the average velocity of the Slave's cratonic lithosphere, as well as the vertical distribution of anisotropy in the upper mantle. The observed high velocities indicate a particularly depleted and/or cold, unperturbed Archean continental lithosphere, and comparisons with other cratonic environments suggest that the Slave craton may be an end member in this respect. This result corroborates those from several petrological studies, which report an ultra-depleted layer of spinel peridotites in the central Slave's upper mantle down to 100–150 km [*Griffin et al.*, 1999], and a cooler mantle in the southeastern Slave than in other Archean cratons [*Kopylova and Caro*, 2004]. Our results also agree with a recent study by *O'Reilly and Griffin* [2006], who used garnet concentrates in xenoliths to infer seismic velocities for the central Slave craton and predicted high *S*-wave velocities comparable to those found here.

[12] Estimates of lithospheric thickness from seismic studies often vary depending on the criteria used to define the lithosphere and asthenosphere. In body-wave tomography, the depth extent of high-velocity regions (i.e., 0.5–2% above global velocity average) in the uppermost mantle has been used to define the extent of the lithosphere [e.g., *Grand*, 1994]. This definition may however overestimate the lithospheric thickness due to vertical smearing. In surface-wave tomography, on the other hand, the base of the lithosphere is inferred from the strongest negative gradient in *S*-wave velocity marking the base of a high-velocity lid [e.g., *Debayle and Kennett*, 2000]. In our *S*-wave velocity profile through Archean stable lithosphere, high velocities of 4.7 ± 0.2 km/s observed from 40–150 km depth are up to 5% higher than global averages (i.e., *ak135*) in this depth range. Below 150 km, we observe a negative gradient that reaches a minimum of ~4.68 km/s at ~275 km depth, consistent with the *ak135* velocity at this depth (within error). If we use the center of the negative velocity gradient to infer the base of the lithosphere, we obtain a depth of 220 ± 65 km. However, reduced depth sensitivity of long period Rayleigh waves prevents us from uniquely resolving structures below ~200 km depth. Therefore, we suggest that the base of the Slave's lithosphere occurs at no less than 150 km, and that a thicker lithosphere that extends to 250 km depth [*van der Lee and Frederiksen*, 2005] cannot be ruled out at this stage. This result agrees well with petrological constraints from xenolith data, which indicate that the base of the Slave lithosphere lies at 160–190 km depth [*Kopylova et al.*, 1999].

[13] Until now, vertical distribution of anisotropy has only been elusively inferred in the Slave craton. *Bank et al.* [2000] suggested a solely sub-lithospheric origin; however, splitting data only provide limited constraints on the vertical extent of anisotropy. Conversely, here we find that anisotropic signatures are robustly observed at most periods between 20–100 s, indicating that anisotropy is present in the lithosphere as well. The anisotropy with APM-parallel fast direction is observed between 29 s and 100 s periods, an interval with greatest depth sensitivity ranging between sub-Moho to lower lithosphere (50–150 km). These results are consistent with those of *Snyder and Lockhart* [2005], who suggested solely on the basis of *SKS* splitting results that the main component of mantle anisotropy may be caused by large-scale, shape-preferred orientation (SPO) geometry within the lithosphere. In their interpretation, this SPO is attributed to a concentration of parallel kimberlite dykes that are aligned with the direction of APM, i.e., perpendicular to the direction of minimum horizontal stress, in which fractures would have opened to accommodate kimberlite dyke intrusions. Our results also indicate variations of anisotropy with period, but due to the broad depth range of surface wave sensitivity kernels, we only suggest the existence of a change in azimuth from a N-S fast direction at short periods

below 29 s to a NE-SW fast direction at longer periods. The shallow N-S trending anisotropy may correspond to regional crustal and uppermost mantle structure resulting from Archean tectonic processes (e.g., sutures) that predated the stabilization of the Slave cratonic lithosphere [*Davis et al.*, 2003]. An independent study by *Snyder and Bruneton* [2007] reached similar conclusions by jointly analyzing *SKS* splitting and Rayleigh wave dispersion data. In this study, the anisotropy results at periods >100 s are less well constrained, but we observe a consistent change in fast direction that may result from APM-oblique asthenospheric flow due to topography at the base of the lithosphere.

[14] In conclusion, this study introduces independent constraints on the vertical structure of the Slave craton. The cratonic root persists to a depth of ~220 km, which is comparable to lithospheric thicknesses found in other Archean cratons, such as Australia [*Simons et al.*, 2002] and Siberia [*Priestley and Debayle*, 2003]. High phase velocities recovered at intermediate periods agree with cooler and/or more depleted lithospheric roots in the Slave craton compared to other Archean cratons. Furthermore, our Rayleigh wave inversion reveals distinct anisotropic domains in the crust, the lithospheric mantle and the sub-lithospheric mantle. The dominant fast direction consistent with the APM of North America reflects the influence of sub-lithospheric flow on almost the entire lithospheric structure.

[15] **Acknowledgments.** We are grateful to Yingjie Yang and Donald Forsyth for many helpful discussions on the inversion method. Constructive reviews by Andrew Frederiksen and an anonymous reviewer helped us improve the manuscript. Thanks to Fiona Darbyshire for generously providing her paper preprint. We also thank members in the NWT Geoscience Centre, BHP-Billiton Diamonds Inc., De Beers Canada Inc., and Tahera Diamond Corp., for logistical support for our field work in the Slave province, and POLARIS consortium for making the data available. This work is funded by NSF grant EAR-0409509 to SR. CWC is partly supported by MIT Fraecis Presidential Fellowship. ESS (Canada) Contribution number 20060733.

References

Bank, C.-G., M. G. Bostock, R. M. Ellis, and J. F. Cassidy (2000), A reconnaissance teleseismic study of the upper mantle and transition zone beneath the Archean Slave craton in NW Canada, *Tectonophysics*, *319*, 151–166.

Bleeker, W., J. W. F. Ketchum, V. A. Jackson, and M. E. Villeneuve (1999), The central Slave basement complex, part I: Its structural topology and autochthonous cover, *Can. J. Earth Sci.*, *36*, 1083–1109.

Bostock, M. G. (1998), Mantle stratigraphy and evolution of the Slave province, *J. Geophys. Res.*, *103*, 21,183–21,200.

Bowring, S. A., T. B. Housh, and C. E. Isachsen (1990), The Acasta gneisses: Remnant of Earth's early crust, in *Origin of the Earth*, edited by H. E. Newsom and J. H. Jones, pp. 319–343, Oxford Univ. Press, New York.

Brune, J., and J. Dorman (1963), Seismic waves and earth structure in the Canadian Shield, *Bull. Seismol. Soc. Am.*, *53*, 167–209.

Darbyshire, F. A., D. W. Eaton, A. W. Frederiksen, and L. Ertolahti (2007), New insights into the lithosphere beneath the Superior Province from Rayleigh wave dispersion and receiver function analysis, *Geophys. J. Int.*, in press.

Davis, W. J., A. G. Jones, W. Bleeker, and H. Grütter (2003), Lithosphere development in the Slave craton: A linked crustal and mantle perspective, *Lithos*, *71*, 575–589.

Debayle, E., and B. L. N. Kennett (2000), The Australian continental upper mantle: Structure and deformation inferred from surface waves, *J. Geophys. Res.*, *105*, 25,423–25,450.

Ekström, G., J. Tromp, and E. W. Larson (1997), Measurements and global models of surface wave propagation, *J. Geophys. Res.*, *102*, 8137–8157.

Forsyth, D. W., and A. Li (2005), Array-analysis of two-dimensional variations in surface wave phase velocity and azimuthal anisotropy in the presence of multipathing interference, in *Seismic Earth: Array Analysis of Broadband Seismograms*, *Geophys. Monogr. Ser.*, vol. 157, edited by A. Levander and G. Nolet, pp. 81–98, AGU, Washington, D. C.

Frederiksen, A. W., M. G. Bostock, and J. F. Cassidy (2001), *S*-wave velocity structure of the Canadian upper mantle, *Phys. Earth Planet. Inter.*, *124*, 175–191.

Grand, S. P. (1994), Mantle shear structure beneath the Americas and surrounding oceans, *J. Geophys. Res.*, *99*, 11,591–11,621.

Griffin, W. L., B. J. Doyle, C. G. Ryan, N. J. Pearson, S. Y. O'Reilly, R. Davies, K. Kivi, E. V. Achterbergh, and L. M. Natapov (1999), Layered mantle lithosphere in the Lac de Gras Area, Slave Craton: Composition, structure, and origin, *J. Petrol.*, *40*, 705–727.

Grütter, H. S., D. B. Apter, and J. Kong (1999), Crust-mantle coupling: Evidence from mantle-derived xenocrystic garnets, in *Proceedings of the Seventh Kimberlite Conference*, edited by J. J. Gurney and S. R. Richardson, pp. 307–313, Red Roof Designs, Cape Town.

Kennett, B. L. N., E. R. Engdahl, and R. Buland (1995), Constraints on seismic velocities in the Earth from traveltimes, *Geophys. J. Int.*, *122*, 108–124.

Kopylova, M. G., and G. Caro (2004), Mantle xenoliths from the southeastern Slave craton: Evidence for chemical zonation in a thick, cold lithosphere, *J. Petrol.*, *45*, 1045–1067.

Kopylova, M. G., J. K. Russel, and H. Cookenboo (1999), Upper-mantle stratigraphy of the Slave craton, Canada: Insight into a new kimberlite province, *Geology*, *26*, 315–318.

Li, A., and K. Burke (2006), Upper mantle structure of southern Africa from Rayleigh wave tomography, *J. Geophys. Res.*, *111*, B10303, doi:10.1029/2006JB004321.

Li, A., D. W. Forsyth, and K. M. Fischer (2003), Shear velocity structure and azimuthal anisotropy beneath eastern North America from Rayleigh wave inversion, *J. Geophys. Res.*, *108*(B8), 2362, doi:10.1029/2002JB002259.

O'Reilly, S. Y., and W. L. Griffin (2006), Imaging global chemical and thermal heterogeneity in the subcontinental lithsopheric mantle with garnets and xenoliths: Geophysical implications, *Tectonophysics*, *416*, 289–309.

Priestley, K., and E. Debayle (2003), Seismic evidence for a moderately thick lithosphere beneath the Siberian Platform, *Geophys. Res. Lett.*, *30*(3), 1118, doi:10.1029/2002GL015931.

Saito, M. (1998), DISPER80: A subroutine package for the calculation of seismic normal-mode solutions, in *Seismological Algorithms: Computational Methods and Computer Programs*, edited by D. J. Doornbos, pp. 293–319, Elsevier, New York.

Simons, F. J., R. D. van der Hilst, J.-P. Montagner, and A. Zielhuis (2002), Multimode Rayleigh wave invsersion for heterogeneity and azimuthal anisotropy of the Australian upper mantle, *Geophy. J. Int.*, *151*, 738–754.

Snyder, D. B., and M. Bruneton (2007), Seismic anisotropy of the Slave craton, NW Canada, from joint interpretation of *SKS* and Rayleigh waves, *Geophys. J. Int.*, *169*, 170–188.

Snyder, D. B., and G. D. Lockhart (2005), Kimberlite trends in NW Canada, *J. Geol. Soc.*, *162*, 737–740.

Tarantola, A., and B. Valette (1982), Generalized non-linear problems solved using the least-squares criterion, *Rev. Geophys.*, *20*, 219–232.

van der Lee, S., and A. Frederiksen (2005), Surface wave tomography applied to the North American upper mantle, in *Seismic Earth: Array Analysis of Broadband Seismograms*, *Geophys. Monogr. Ser.*, vol. 157, edited by A. Levander and G. Nolet, pp. 67–80, AGU, Washington, D. C.

Weeraratne, D. S., D. W. Forsyth, K. M. Fischer, and A. A. Nyblade (2003), Evidence for an upper mantle plume beneath the Tanzanian craton from Rayleigh wave tomography, *J. Geophys. Res.*, *108*(B9), 2427, doi:10.1029/2002JB002273.

C.-W. Chen and S. Rondenay, Department of Earth, Atmospheric, and Planetary Sciences, Massachusetts Institute of Technology, 77 Massachusetts Avenue, Cambridge, MA 02139, USA. (cwchen@mit.edu)

D. B. Snyder, Geological Survey of Canada, 615 Booth Street, Room 204, Ottawa, ON, Canada K1A 0E9.

D. S. Weeraratne, Department of Terrestrial Magnetism, Carnegie Institution of Washington, 5241 Broad Branch Road NW, Washington, DC 20015, USA.